ISSN: 2710-0588

Numerical Simulation of Different Ventilation Methods in Small Meeting Rooms

Yiting Zheng

School of Civil Engineering, Central South University of Forestry and Technology, Changsha 410004, China

Abstract

For a long time, conference rooms have served as vital workplaces where indoor air quality directly impacts the physical and mental well-being as well as work efficiency of occupants. Therefore, selecting a ventilation method that simultaneously meets human comfort and indoor air quality requirements while achieving energy-saving objectives is particularly crucial. This paper employs Fluent software and computational fluid dynamics (CFD) analysis to simulate and analyze the velocity field distribution within different ventilation configurations for conference rooms, providing a theoretical basis for creating optimal indoor environments.

Keywords

Calculate fluid dynamics, velocity distribution, airflow organization.

1. Introduction

As living standards improve, people's expectations for indoor work environments continue to rise [1]. Creating a favorable indoor environment is more conducive to people's physical and mental well-being. Therefore, maintaining a healthy indoor air environment is the primary prerequisite for interior design. The indoor air environment encompasses both thermal-humidity conditions and air quality, with proper ventilation serving as the fundamental guarantee for both. The primary purpose of ventilation is to enhance indoor air quality and thereby foster a favorable working environment. Consequently, rational ventilation methods represent an inevitable requirement for the advancement of modern air conditioning technology [2]. Air exchange ventilation not only provides effective airflow organization and creates a comfortable thermal and humidity environment, but also offers economic and energy-efficient benefits, making it an ideal ventilation solution. In such small spaces, where soundproofing requirements necessitate strong sealing, improper ventilation conditions can easily lead to elevated indoor CO_2 levels and poor air quality. This may cause symptoms like chest tightness and breathing difficulties, thereby impacting personnel productivity [3]. Due to the limited understanding and insufficient experience among China's design and engineering personnel regarding displacement ventilation systems, the application of displacement ventilation technology remains relatively uncommon in China [4]. By introducing fresh air and expelling contaminated air, indoor pollutant concentrations are reduced and thermal comfort is improved. Different ventilation methods and airflow patterns yield varying degrees of dilution and removal of indoor pollutants, resulting in differing air quality perceptions among occupants. Consequently, research into diverse ventilation approaches is particularly crucial. Given the characteristics of such micro-spaces, researching optimal airflow organization—including supply air patterns, indoor temperature and humidity, and air velocity—can significantly improve air quality and mitigate local thermal discomfort within these confined areas. This approach reduces energy consumption and promotes environmental sustainability [5].

ISSN: 2710-0588

2. Model Development

2.1. Geometry Modeling

This study focuses on small conference rooms, drawing reference from the design of a fifth-floor conference room at a school in Changsha. To enhance computational efficiency in numerical simulations, the conference room was simplified and modeled using AutoCAD 2019 software, as shown in Figure 1. The geometric model measures 5 meters in length, 4 meters in width, and 3.3 meters in height, meeting design specifications. Its interior features a conference table (1.5m × 2.7m × 0.8m), an air conditioner (0.5m × 1.7m × 0.3m), a door (0.9m × 2.4m), and a window (2.4m × 1.8m, with a sill height of 0.9m). The upper opening of the air conditioner serves as the air intake, while the lower opening functions as the exhaust vent, both measuring 0.4m × 0.3m.

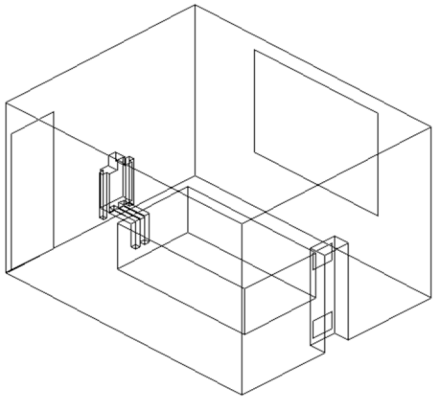

Figure 1. Geometric Model of Conference Room

2.2. Mesh Generation

Import the 3D model into ICEM in SAT format for mesh generation. Currently, computational meshes can be broadly categorized into structured and unstructured meshes. This study employs an unstructured mesh for model meshing. The number of mesh elements influences both computational accuracy and processing time, as illustrated in Figures 2 and 3. The constructed model was then imported into Fluent, where the differential equations were discretized using the finite volume method. The pressure-velocity coupling employed the SIMPLE algorithm. For all solved discretized equations except the energy equation, the root mean square residual (RMSR) convergence criterion was set to, while the energy equation's RMSR convergence criterion was set to. Assuming the indoor air is an incompressible fluid, the Boussinesq approximation is employed to account for thermal buoyancy effects.

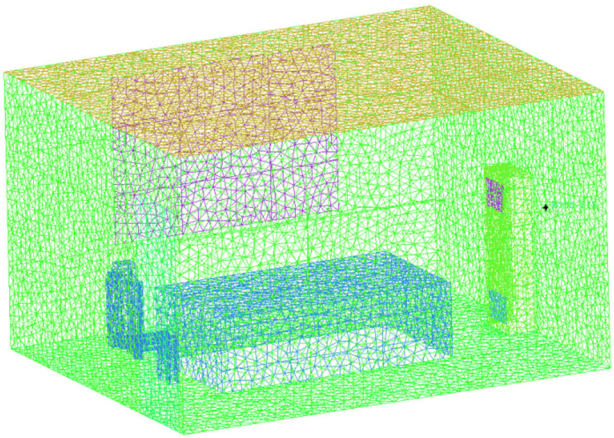

Figure 2. Schematic Diagram of mesh Partitioning

ISSN: 2710-0588

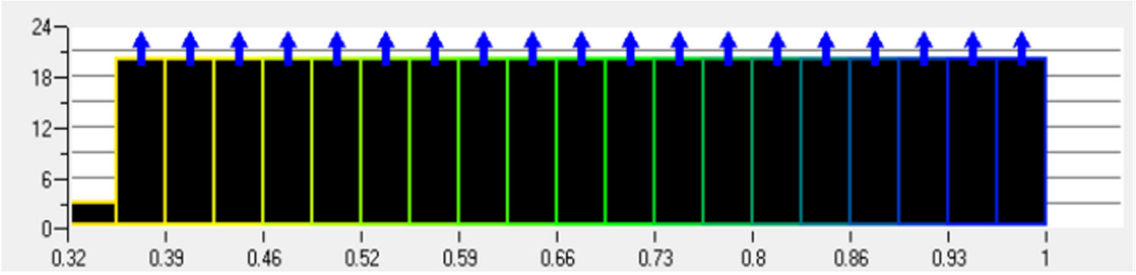

Figure 3. Mesh Quality Statistics Chart

2.3. Define Boundary Conditions

This study on small conference rooms uses summer cooling conditions as the basis for calculations. As shown in Figure 4, (a) For Type I, the supply air temperature is set to 18°C, with the supply air outlet configured as a velocity inlet boundary condition at 3 m/s; (b) For Type II, the window type is set to Velocity Inlet, and the door type is set to outflow. The indoor air flow satisfies the Boussineq assumption [9]; that is, variations in air density affect only the buoyancy force term in the momentum equation, while the density remains constant for all other terms. The room is well-sealed, and the influence of natural infiltration airflow is neglected.

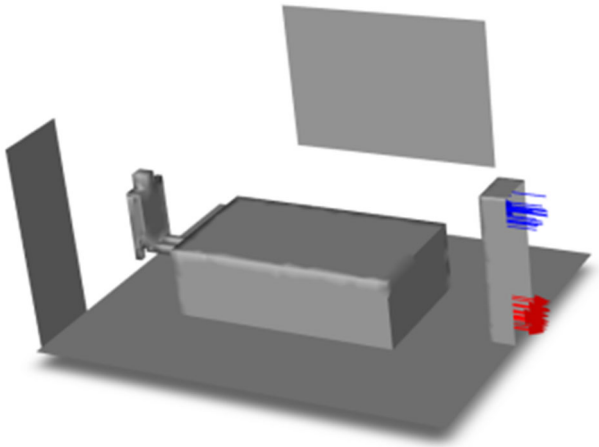

Figure 4. (a) Air-conditioning ventilation system

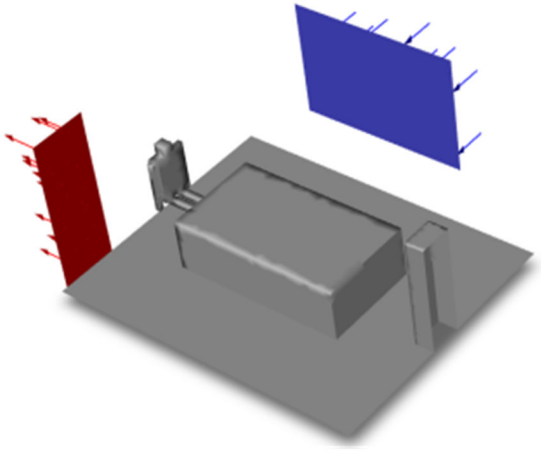

Figure 4. (b) Door and window ventilation system

ISSN: 2710-0588

3. Numerical Model Theory

3.1. Governing Equations of Fluid Dynamics

3.1.1. Equation of Conservation of Mass

The fundamental set of equations describing fluid motion is known as the fluid dynamics equations, comprising the conservation equations for mass, momentum, and energy. The mass conservation equation, also known as the continuity equation [6-10], states that the increase in fluid mass per unit time equals the net mass inflow into a fluid element during the same time interval. The equation is expressed as follows:

$$\frac{\partial \rho}{\partial t} + div(\rho \vec{u}) = 0 \tag{1}$$

In the equation: ρ denotes fluid density, kg/m^3; t represents time, s; v is fluid velocity, m/s. At low flow velocities, the fluid is considered incompressible. For constant incompressible fluids, density variations can be neglected and treated as constant. The above equation can be simplified to:

$$div(\rho \vec{u}) = 0 \tag{2}$$

3.1.2. Equation of Conservation of Momentum

The law of conservation of momentum, also known as the Navier-Stokes equation, states that the sum of all external forces acting on a small element

equals the rate of change of the fluid's momentum within that element relative to time [6-10]. Its expression is as follows:

$$\begin{cases} \frac{\partial(\rho \vec{u})}{\partial t} + div(\rho \vec{uu}) = -\frac{\partial P}{\partial x} + div(\eta \cdot grad\vec{u}) + S_x \\ \frac{\partial(\rho \vec{v})}{\partial t} + div\left(\rho \vec{vu}\right) = -\frac{\partial P}{\partial y} + div(\eta \cdot grad\vec{v}) + S_y \\ \frac{\partial(\rho \vec{z})}{\partial t} + div\left(\rho \vec{zu}\right) = -\frac{\partial P}{\partial z} + div(\eta \cdot grad\vec{z}) + S_z \end{cases} \tag{3}$$

In the equation: P denotes fluid pressure, Pa;ηrepresents fluid dynamic viscosity, N·s/m^2.

3.1.3. Equation of Conservation of Energy

The law of conservation of energy, also known as the first law of thermodynamics, states that the increase in the internal energy of an object equals the sum of the heat absorbed by the object and the work done on the object [6-10]. Its mathematical expression is as follows:

$$\frac{\partial(\rho I)}{\partial t} + div(\rho I \vec{u}) = div\left(k \cdot grad\vec{T}\right) - P \cdot div\left(\rho \vec{U}\right) + \Phi + S_I \tag{4}$$

In the equation: I represents the internal energy of the fluid, J; k denotes the thermal conductivity, W/ (m · K); T is the fluid temperature, K; Φ indicates the dissipation function of the fluid; represents the heat source within the fluid. For an incompressible ideal gas, the fluid density ρ remains constant, and I = h · T. The above equation can be simplified to:

ISSN: 2710-0588

$$\frac{\partial(T)}{\partial t} + div(T\vec{u}) = div\left(\frac{k}{\rho C_P} \cdot grad\vec{T}\right) + \frac{S_T}{\rho} \tag{5}$$

3.2. Turbulence Model

The fundamental principle of turbulence models lies in establishing a functional relationship between the turbulence-averaged time parameter and the turbulence viscosity coefficient [8]. Turbulence models commonly employed in practical applications include the zero-equation model, standard k-ε model, low Reynolds number k-ε model, and refined non-linear (RNG) k-ε model . Given the standard k-ε model's broad applicability and adequate computational accuracy, this study employs FLUENT software to simulate and analyze the ventilation conditions within the conference room. The standard k-ε turbulence model is a turbulence model based on the transport equations for turbulent kinetic energy k and dissipation rate ε. The transport equation for k is derived from precise mathematical-physical equations, while the transport equation for ε is established based on physical reasoning [11]. The equations for k and ε are as follows:

$$\frac{\partial(\rho k)}{\partial t} + \frac{\partial(\rho u_i k)}{\partial x_i} = \frac{\partial}{\partial x_j}\left[\left(\mu + \frac{\mu_t}{\sigma_\varepsilon}\right)\frac{\partial k}{\partial x_j}\right] + G_k + G_b - \rho\varepsilon + S_k \tag{6}$$

$$\frac{\partial(\rho\varepsilon)}{\partial t} + \frac{\partial(\rho u_i \varepsilon)}{\partial x_i} = \frac{\partial}{\partial x_j}\left[\left(\mu + \frac{\mu_t}{\sigma_\varepsilon}\right)\frac{\partial k}{\partial x_j}\right] + G_{l\varepsilon}\frac{\varepsilon}{k}(G_K + C_{3\varepsilon}G_b) - C_{2\varepsilon\rho}\frac{\varepsilon^2}{k} + S_\varepsilon \tag{7}$$

$$\mu_t = \rho C_\mu \frac{k^2}{\varepsilon} \tag{8}$$

In the equation: G_k represents the turbulent kinetic energy generated by the mean velocity gradient; G_b represents the turbulent kinetic energy induced by buoyancy forces; $C_{1\varepsilon}$, $C_{2\varepsilon}$, $C_{3\varepsilon}$, and C_μ denote empirical constants; σ_k and σ_ε represent the turbulent Prandtl numbers for k and ε, respectively; S_k and S_ε are custom source terms.

4. Analysis of Simulation Results for Different Ventilation Methods

After performing numerical simulations based on the boundary conditions derived from the analysis, the simulation results undergo post-processing. The effects of different airflow organization methods on the indoor thermal environment and air quality are compared, and representative cross-sections are selected from the post-processing results for comparative analysis. As shown in Figure 5, two cross-sections at X=0.3m and X=1.6m were selected for comparison in the X-direction to analyze the temperature and velocity fields at these sections. In the Z-direction, a cross-section at Z=2.1m was chosen, positioned at the supply air duct location and coinciding with the return air grille section. Under specified constraints, design the supply air pattern. Based on the validation results of the turbulence model discussed earlier, CFD simulations were conducted using the standard k-ε turbulence model for different airflow organization configurations. Analysis of the resulting indoor velocity field distributions revealed that varying supply air patterns significantly influence indoor airflow organization, thereby affecting occupant comfort and indoor air quality. Figure 5 (b) shows the ventilation

ISSN: 2710-0588

mode where fresh air enters the room at a low velocity from the east wall. Part of the supplied fresh air is obstructed by desks, forming a counterclockwise vortex along the west wall. (c) Compared to (e), it is evident that the door and window ventilation configuration affects a larger area of indoor airflow with higher wind speeds, resulting in a noticeable draft sensation on occupants.

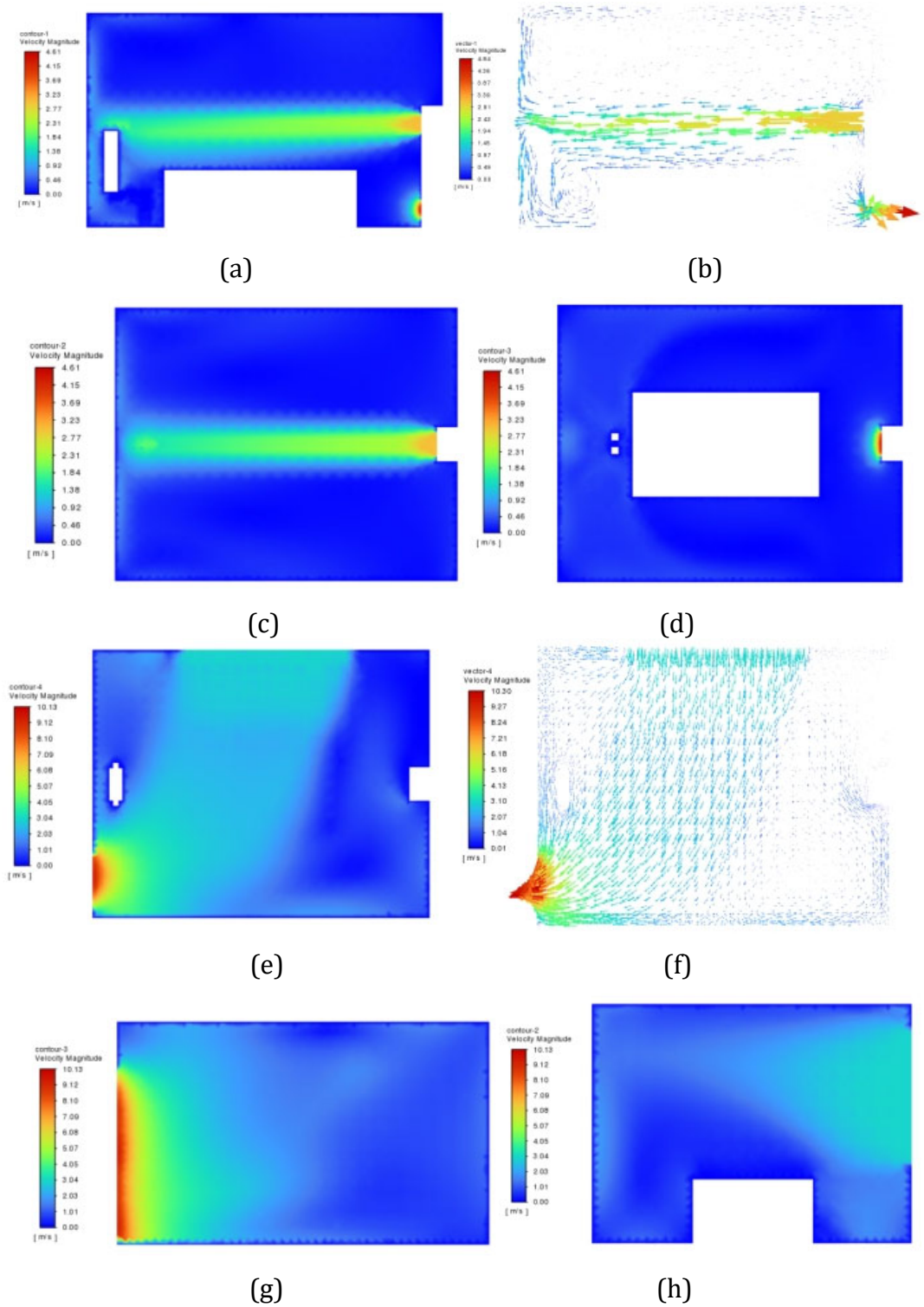

Figure 5. Velocity Distribution Diagram for Different Cross-Sections of Airflow Organization Patterns

ISSN: 2710-0588

5. Conclusion

To investigate the rationality of airflow organization in small spaces, improve thermal comfort and air quality conditions within them, and understand occupant comfort during use. This paper focuses on the design of airflow organization patterns in small spaces occupied by people. Taking a small conference room as an example, Fluent software was used to simulate the velocity field distribution within different ventilation zones. Multiple turbulence models were simulated and validated. Comparing the simulated values with experimental data revealed that the zero-equation model exhibited significant deviation when simulating indoor airflow organization. while the standard k-ε model and RNG k-ε model showed broadly similar trends. For computational convenience, the standard k-ε model was selected for this numerical simulation study. Due to incomplete mastery of the operational procedures during the preliminary phase, the simulation experiment lacked sufficient control variable groups, resulting in insufficient data support for the experiment. Further research could investigate window dimensions and positions, or the placement of exhaust vents at different locations within the air conditioning system (e.g., upper side exhaust, middle side exhaust, lower side exhaust, single-side exhaust).

References

[1] Tsinghua University Building Energy Efficiency Research Center: Annual Development Research Report on China's Building Energy Efficiency. (China Architecture & Building Press, China, 2020).

[2] Tsinghua University Building Energy Efficiency Research Center: Annual Development Research Report on China's Building Energy Efficiency. (China Architecture & Building Press, China, 2023).

[3] M. Salmanzadeh, G. Zahedi, G. Ahmadi, et al. Comutational modeling of effects of thermal plume adjacent to the body on the indoor airflow and particle transport. Journal of Aerosol Science, vol.53(2012), p. 29-39.

[4] J.J. An, D. Yan, X. Zhou, et al. Simulation Analysis of the Differences in Indoor Environment Creation Between Mechanical Ventilation and Natural Ventilation in Office Buildings. (Architectural Science, China, 2015).

[5] R.W. Yan, Y. Wang: The Impact of Ventilation Modes on Indoor Air Quality and Comfort in Offices. (Journal of Lanzhou Jiaotong University, China), vol.37(2018) No.6, p.92-98.

[6] Y. Nakamura, T. Oke and R. Wind, temperature and stability conditions in an east-west oriented urban canyon. Atmospheric Environment, vol.22(1988) No.12, p. 2691-2700.

[7] D. Rim, L. Wallace, S. Nabinger, et al. Reduction of exposure to ultrafine particles by kitchen exhaust hoods: the effects of exhaust flow rates, particle size, and burner position. Science of the Total Environment, vol.432(2012), p. 350-356.

[8] Coello R, Charlett A, Wilson J, et al. Adverse impact of surgical site infections in English hospitals. Journal of Hospital Infection, vol.60(2005) No.2, p. 93-103.

[9] Risto Kosonen. Indoor air pollution due to chipboard used as a construction material . Atmospheric Environment, vol.9(2006) No.12, p. 1121-1127.

[10] A.C.K. Lai, Y.W. Ho: Spatial concentration variation of cooking-emitted particles in a residential kitchen. Building and Environment, vol.43(2007) No.5, p. 86-88.

[11] E.Y. Chen: Research on Discrete Finite Element Numerical Methods and Numerical Simulation of Complex Impact Flow Fields. (Nanjing University of Science and Technology, China, 2008).